Research Article

Nano Biomed Eng

Optical and Paper-based Dual Sensing of Hg^{2+} and Colorimetric Reduction of Cr(VI) by Green Synthesized Silver Nanoparticles Prepared from the Bark Extract of *Sweetinia mahagoni* and Their Promising Antimicrobial Applications

Hema Gunti[1], Susmila Aparna Gaddam[2], Ramamurthy Nadipi[3], Venkata Subbaiah Kotakadi[4]

[1] Department of Biotechnology, Maharani's Science College for Women, Maharani Cluster University, Bangalore, India
[2] Department of Virology, Sri Venkateswara University, Tirupati, India
[3] Department of Botany, PVKN Government College, Chittor, India
[4] DST-PURSE Center, Sri Venkateswara University, Tirupati, India

Corresponding author. E-mail: kotakadi72@gmail.com

Received: Jan. 10, 2023; **Revised:** Mar. 13, 2023; **Accepted:** Mar. 27, 2023

Citation: H. Gunti, S.A. Gaddam, R. Nadipi, et al. Optical and paper-based dual sensing of Hg^{2+} and colorimetric reduction of Cr(VI) by green synthesized silver nanoparticles prepared from the bark extract of *Sweetinia mahagoni* and their promising antimicrobial applications. *Nano Biomedicine and Engineering*, 2023.

http://doi.org/10.26599/NBE.2023.9290012

Abstract

This study was conducted to identify promising applications of green silver nanoparticles (AgNPs) prepared from a bark extract of *Sweetinia mahagoni* (Sm). The green synthesized Sm-AgNPs were characterized using various spectroscopy methods. AgNPs were first investigated using ultraviolet–visible spectroscopy, and the metal nanoparticles exhibited an intense surfaceplasmon resonance (SPR) peak at different wavelengths. The green synthesized Sm-AgNPs had an SPR peak at 430 nm, which confirms the formation of Sm-AgNPs. In addition, Fourier transform infrared (FTIR) spectroscopy was conducted to determine the bioactive compounds of bark extract that actively participate in the reduction of Sm-AgNPs, and the results revealed O—H stretching of free hydroxyl alcohol and phenols, N—H bonds of primary amines, S＝O stretching of sulfoxide in aromatic groups, C—I stretching due to aliphatic iodo compounds, and C—Br stretching by halo compounds of the bark extract which might reduce and stabilize Sm-AgNPs. Scanning electron microscopy (SEM) and energy dispersive X-ray spectroscopy (EDS) results revealed that Sm-AgNPs were approximately irregular spheres. EDS results revealed the complete reduction of silver to elemental silver. The particle size analysis of Sm-AgNPs was conducted using dynamic light scattering (DLS), and the results revealed that Sm-AgNPs were polydisperse with an average size range from 35.8 to 47.8 nm, an average mean size of 41.3 nm, and a *Z* average of 37.7 nm. Sm-AgNPs had a negative zeta potential value of −19.0 mV, indicating that Sm-AgNPs were very stable in colloidal form. Further studies were carried out to demonstrate their usefulness in industrial and biomedical applications. In these studies, Sm-AgNPs exhibited a very good antibacterial activity against both Gram-negative and Gram-positive bacteria. In addition to regular assays, we also investigated important industrial applications such as the reduction of toxic hexavalent chromium to a nontoxic form and sensing of Hg^{2+} ions. The results revealed that Sm-AgNPs had an excellent performance in biosensor applications such as sensing and detecting mercury at parts per million/parts per billion levels. In conclusion, green Sm-AgNPs are promising materials in therapeutic and industrial applications.

Keywords: green Sm-AgNPs; spectral characterization; antibacterial activity; chromium reduction and detection; dual sensing of mercury; optical method; paper-based bio-sensing

Introduction

The towering industrial development in the past twenty years has resulted in environmental pollution due to industrial waste and toxic elements, and researchers actively focus on this major problem. These contaminants are the main etiology of several human diseases and disorders. These toxic elements are also a major cause of contamination of soil and water resources. Furthermore, the agricultural crops growing in these contaminated soils cause gastrointestinal problems, anemia, and skin disorders [1–3]. According to the World Health Organization (WHO), the maximum concentration of Cr(VI) should not exceed 0.05 mg/L [4]. Cr(VI) is highly toxic in nature and induces carcinogenic and mutagenic changes in humans, leading to cancer and other disorders, which is confirmed and evaluated by the International Agency for Research on Cancer [5]. Environmental pollution caused by chromium (Cr(VI)) accumulation in water bodies and soil is a problem for various industries (e.g., chemicals, leather tanning, chrome plating, wood preservation, alloy manufacturing, and dye manufacturing), applications and products [6]. Therefore, scientists must work on how to reduce Cr(VI) contamination to preserve a suitable habitat for humans. Researchers have investigated a variety of methods using nanotechnology to reduce Cr(VI) to Cr(III), since Cr(III) is believed to be less toxic in nature, has a poor fluidity, easily precipitates in the presence of various natural adsorbents, and is easily reduced by various metal nanoparticles.

Another major environmental problem is the accumulation of mercury in water and soil, which can lead to major health problems in humans and animals. Mercury is highly soluble in water and exists primarily on the water surface. Once mercury enters an aquatic ecosystem, this toxic element accumulates in the food chain in the form of methyl mercury (a neurotoxin), especially in edible fishes, causing prenatal brain damage, various cognitive and motion disorders, and the deadly Minamata disease [7]. According to the WHO, the maximum permissible level of mercury in drinking water is 1 µg/L. Thus, excess intake of mercury can cause serious health problems in humans due to its extremely toxic nature, such as damage to the brain, kidneys, immune system, and nervous system [8]. Therefore, monitoring the mercury ions in aqueous water bodies is highly important for environmental protection. Different advanced analytical instruments are available for mercury (Hg^{2+}) detection, such as inductively coupled plasma-optical emission spectroscopy (ICP-OES), inductively coupled plasma-mass spectroscopy (ICP-MS), and high performance liquid chromatography (HPLC), as well as old analytical instruments such as atomic absorption spectroscopy (AAS) and gas chromatography-mass spectroscopy (GC-MS) [9–12]. Although these instruments are sophisticated, the detection of mercury is very expensive and requires skilled personnel to operate, thus these experiments are not suitable for field operation. Hence, a simple, rapid, affordable, and highly sensitive method or device for the detection of mercury is still needed.

Nanotechnology has been an emerging research area in the last two decades, and these technologies have resulted in the development of a wide range of optical and electrochemical sensors for the detection of mercury [13–16]. These technologies are better than conventional tools due to their low cost of analysis, shorter analysis time, field readiness, high specificity, and ultra-sensitivity. Silver nanoparticles (AgNPs) have gained more attention for mercury sensor development among the nanomaterials [17–19]. During the past decade, scientists have developed numerous AgNP-based colorimetric sensing modalities for the detection of mercury [20]. AgNPs have been used in combination with chemicals or bio-chemicals to conduct mercury sensing. An anti-aggregation-based colorimetric sensor was designed for the detection of mercury ions by the addition of 6-thioguanine during the assay [21], and the addition of

thiol compounds, such as cysteine [22] and dithiothreitol (DTT) [23, 24], was also used for mercury sensing. Nain et al. [16] developed a simple dual mechanism-based approach for the sensing of mercury by capping AgNPs with glucose and developed a paper-based sensor.

The present study investigated the green synthesis of AgNPs using the aqueous bark extract of *Swietenia mahagoni* (L.) Jacq (Sm). *S. mahagoni* (L.) Jacq. (West Indian mahogany) belongs to the family Meliaceae. This important plant is native to tropical and subtropical regions. Although this plant originated from the Caribbean, Asian countries, Mexico, and Central and South American countries presently cultivate the plant. Three species have been identified based on geographical distribution, *S. mahagoni* (L.) Jacq., *S. humilis* Zucc. (Pacific coast mahogany), and *S. macrophylla* King (Honduran mahogany) [25]. *S. mahagoni* is a medicinally important plant according to Indian Ayurveda and has been widely used as a folk medicine to treat different diseases. According to the review of earlier studies, mahogany plants have a vast range of pharmacological activities such as antimicrobial, antioxidant, analgesic, anti-inflammatory, hepatoprotective, antiulcer, anti-diabetic, anti-human immunodeficiency virus (HIV), immunomodulator, insect repellent and larvicidal, antifungal, depressant, anticonvulsant and neuropharmacological, platelet aggregation inhibitors, antidiarrheal, antimutagenic, and anticancer [26–28]. The isolated phytochemical content from the seeds, bark, twigs, leaves, and stems of *S. mahagoni* is flavonoids, anthraquinones, phospholipids, alkaloids, phenols, saponins, terpenoids, cardiac glycosides, volatile oils, and long chain unsaturated acids. This plant contains more than 45 limonoids such as swietenolide, swiemahogins A and B, andirobin, mexicanolide, 2-hydroxy-3-O-tigloylswietenolide, gedunin, phragmalin, triterpenes, tetranortriterpenes, swietenine, dimeric triterpenoid, and chlorogenic acid, and heavy metal phytoremediation activity has also been reported [29, 30]. The important bioactive constituents of *Swietenia* bark from aqueous and methanol extracts, which include flavonoids, triterpenoids, alkaloids, and phenolics, are known to have antidiabetic activity.

In view of the mammoth medicinal importance of *S. mahagoni*, the present research study was conducted to develop the green synthesis of AgNPs using bark extract, to characterize this material with various techniques such as ultraviolet–visible (UV–Vis) absorbance, Fourier transform infrared (FTIR) spectroscopy, dynamic light scattering (DLS), zeta potential, scanning electron microscopy (SEM), and energy dispersive X-ray spectroscopy (EDS), and to study the biomedical and industrial applications of this material. The biosynthesis of metal nanoparticles using the bark extract of *S. mahagoni* has not been studied thus far. Green synthesis of AgNPs and other metal nanoparticles has been widely carried out for the past two decades due to their simple, efficient, and environmentally safe processes that avoid external toxic chemicals. These green AgNPs fabricated with different parts of plants have various important biomedical and industrial applications. Fabricated AgNPs have been used in the diagnosis of disease, detection of nuclear acids, and agriculture and food industries, as well as biosensor, optical, and electrochemical applications [31–34]. AgNPs also have a large surface area, tunable size, excellent catalytic activity, and superior antimicrobial and anticancer properties [35–37].

Materials and Methods

Materials and chemicals

We used silver nitrate (Sigma-Aldrich, Munich, Germany), mercuric chloride (Qualigens, Waltham, MA, USA), chromium(VI) (Sigma-Aldrich), nutrient agar, nutrient broth (Himedia, Mumbai, India), potassium bromide (Sigma-Aldrich), antibiotic discs (Himedia), glassware (Borosil, Mumbai, India), and Whatman No. 1 filter paper (Maidstone, UK) in our experiments. *S. mahagoni* tree bark (Fig. 1) was collected from the plantation area of Sri Venkateswara Veterinary University campus, Tirupati, Andhra Pradesh, India.

Preparation of the *S. mahagoni* bark extract

Fresh bark was collected from an *S. mahagoni* tree, brought to the laboratory, rinsed with tap water followed by distilled water, and cut into small pieces. Bark pieces were weighed, and 5 g of bark was added to 150 mL of Milli-Q water (MilliporeSigma, Burlington, MA, USA) and heated in a water bath for 30 min at 70 °C. The bark extract was cooled, incubated overnight at room temperature, and filtered through Whatman No. 1 filter paper. The filtrate was collected and stored at 4 °C for further experiments.

Fig. 1 (a) *S. mahagoni* tree, **(b)** tree trunk, and **(c)** tree bark.

Green synthesis of AgNPs

Aqueous 1 mmol/L silver nitrate ($AgNO_3$) was prepared using Milli-Q water and stored at room temperature in an amber reagent bottle. A diluted 0.2 mmol/L $AgNO_3$ solution was used for the green synthesis. 5 mL of diluted filtrate of *S. mahagoni* bark extract was added to 10 mL of 0.2 mmol/L $AgNO_3$ solution to reduce Ag^+ ions and form AgNPs. The filtrate acted as a reducing and stabilizing agent for the reduction of 0.2 mmol/L $AgNO_3$. The samples were incubated at room temperature until the color of solution changed from colorless to brown and subsequently dark brown, as shown in Fig. 2. The current study demonstrated that the green synthesis of Sm-AgNPs using a bark extract of *S. mahagoni* was possible without toxic and hazardous chemicals.

Purification of Sm-AgNPs

The solution containing Sm-AgNPs was centrifuged at 10 000 r/min for 20 min to obtain green Sm-AgNPs pellets. The Sm-AgNPs pellets were re-dispersed in 15 mL of Milli-Q water and centrifuged again at 10 000 r/min for 20 min to remove any unbound plant molecules. The centrifugation and re-dispersion in Milli-Q water were repeated thrice to obtain pure green Sm-AgNPs that were free of unbound plant extract residues. The purified green Sm-AgNPs pellets were then used to conduct particle size analysis, zeta potential analysis, SEM, and EDS.

Spectral characterization of Sm-AgNPs

Green synthesized Sm-AgNPs, as well as the bark extract of *S. mahagoni*, were analyzed by UV–Vis absorbance spectroscopy within the wavelength range of 220–750 nm using a NanoDrop 8000 (Thermo Fisher Scientific, Waltham, MA, USA) UV–Vis spectrophotometer available at the DST-PURSE Center, Sri Venkateswara University, Tirupati, India. Green synthesized Sm-AgNPs were analyzed at room temperature using the NanoDrop 8000 spectrophotometer at a resolution of 1 nm to detect the surface plasmon resonance (SPR) of green

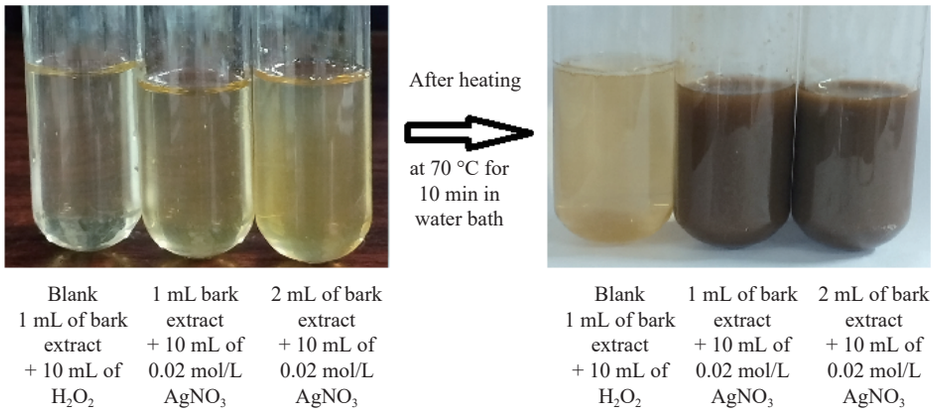

Fig. 2 The color change of *S. mahagoni* bark extract, 1 mL of bark extract + 10 mL of 0.02 mol/L silver nitrate, and 2 mL of bark extract + 10 mL of 0.02 mol/L silver nitrate after a 70 °C water bath for 10 min.

synthesized AgNPs. FTIR analysis of *S. mahagoni* bark extract and green synthesized Sm-AgNPs was conducted using a Bruker Tensor 27 (Billerica, MA, USA) at the Department of Physics, Sri Venkateswara University, Tirupati, India to detect which bioactive phyto-constituents were present in the bark extract and involved in the bio-reduction and capping of green synthesized Sm-AgNPs. Particle size and zeta potential analyses of green synthesized Sm-AgNPs were conducted using DLS with a Nanopartica SZ-100 instrument (Horiba, Kyoto, Japan) available at the DST-PURSE Center to determine the size distribution of Sm-AgNPs in the purified aqueous sample and stability of green synthesized Sm-AgNPs in the aqueous colloidal solution. SEM and EDS were conducted using an Oxford Inca Penta FeTX3 EDS instrument (Abingdon, UK) attached to a Carl Zeiss EVO MA 15 scanning electron microscope (200 kV, Oberkochen, Germany) with a line resolution of 2.32 Å available at the RUSA-SEM facility (Yogi Vemana University, Kadapa, India). These images were obtained by drop coating a drop of Sm-AgNPs on glass pieces cut to uniform sizes. An energy dispersive absorption spectroscopy photograph of Sm-AgNPs was obtained using the SEM equipment mentioned above.

Antibacterial activity of Sm-AgNPs

Bacterial strains of the microorganisms *Escherichia coli* (Gram-negative), *Klebsialla pneumonia* (Gram-negative), *Pseudomonas aeruginosa* (Gram-negative), *Staphylococcus aureus* (Gram-positive), and *Bacillus megaterium* (Gram-positive) were obtained from the Department of Microbiology and Department of Biochemistry and maintained at the DST-PURSE Center, Sri Venkateswara University, Tirupati, India; these strains were used to determine the antibacterial activity of Sm-AgNPs and that of the bark extract of *S. mahagoni*. The above bacterial strains were maintained on nutrient agar slants, and subcultures were freshly prepared in nutrient broths before use. Bacterial cultures were prepared by transferring a single colony into a tube containing 20 mL of nutrient broth and grown overnight at 37 °C in a shaking incubator. The antibacterial activities of Sm-AgNPs and the bark extract of *S. mahagoni* were determined using four different bacterial strains, *E. coli*, *P. aeruginosa*, *S. aureus*, and *B. megaterium*, and the Kirby Bauer disc diffusion method. The procedure was followed according to Kotakadi et al [38, 39]. Bacterial cultures of the above bacteria were prepared, 100 µL of these cultures were spread on nutrient agar plates, and then sterile Whatman Grade 1 filter paper discs were placed on the nutrient agar plates. The amounts of bark extract of *S. mahagoni* and green synthesized Sm-AgNPs deposited on the sterile discs were 20 and 40 µg, respectively. Amoxyclav (30 µg, Himedia SD063) discs were used as the standard antibiotic. Nutrient agar plates loaded with the bark extract of *S. mahagoni*, Sm-AgNPs, and antibiotic were incubated at 37 °C overnight. In the next day, the zone of inhibition (ZOI) was calculated, and photographs were acquired for further analysis.

Colorimetric detection of Cr(VI) by green Sm-AgNPs

Reduction of chromium (Cr(VI)) by green synthesized Sm-AgNPs was chosen to quantify the catalytic activity [40]. The colorimetric detection of Cr(VI) was carried out by adding 350 µL of Cr(VI) to 650 µL of freshly prepared Sm-AgNPs and observed for instant coloration or color change. The reaction mixture was mixed thoroughly and its absorption spectrum was recorded using the above mentioned NanoDrop 8000 spectrophotometer in the range of 220–750 nm with a 1 cm path length.

Colorimetric sensor for the detection of Hg^{2+} ions using green Sm-AgNPs

The colorimetric detection of Hg^{2+} ions was conducted using green synthesized Sm-AgNPs. The reaction was carried out as follows: 200 µL of Sm-AgNPs stock solution, 300 µL of Milli-Q water, and 500 µL of Hg^{2+} solution were added to form a reaction mixture. The resulting reaction mixture was equilibrated by stirring on a Vortex machine for an optimum incubation time and then the UV–Vis spectrum in the wavelength range of 200–800 nm was recorded. The protocol was previously described by Vasileva et al [41].

Paper-based sensor detection of Hg^{2+} ions using green Sm-AgNPs

To develop a paper-based colorimetric sensing strip for Hg^{2+} detection, 5 µL of a green synthesized colloidal solution of Sm-AgNPs was added to Whatman filter paper No. 1 (pore size is 11 µm) at eight different spots and then dried at room temperature for 15 min. These Sm-AgNP-immobilized paper strips were used for mercury detection. For this experiment, mercury solutions of

varying concentrations (100, 50, 10, and 1 mmol/L) and (100, 50, 10, and 1 μmol/L) were dispensed shot-wise (shot volume is 5 μL) at an interval of 1 min on four different Sm-AgNP spots in the sensing test line (T line) until spot discoloration was observed. The volume of mercury solution consumed to achieve discoloration of the Sm-AgNP spot was noted for all the concentrations. For the control experiments, deionized (DI) water, i.e., an equivalent volume of mercury solution consumed to achieve discoloration of the spot, was added to the Sm-AgNP spot in a shot-wise fashion (shot volume is 1 μL) in the control line (C line). The experiment was done according to the protocol of Nain et al. [16] with a slight modification suitable to our lab conditions.

Results and Discussion

UV–Vis spectral analysis of Sm-AgNPs

The detection of green synthesized AgNPs and other metal nanoparticles can be easily analyzed via UV–Vis spectroscopy. In this study, the results revealed that the bark extract of *S. mahagoni* reduced the 0.2 mol/L silver nitrate solution to an ionic form of Ag^{+}. This reduction is visually confirmed by the colorless reaction solution changing to a dark brownish color (Fig. 2). The green synthesized AgNPs, thus named as Sm-AgNPs, consists of free electrons, which gives rise to the SPR absorption peak present in the UV–Vis spectral analysis. The SPR peak of green synthesized Sm-AgNPs was obtained at 430 nm (Fig. 3). Metal nanoparticles can be synthesized by various physical and chemical methods using organic chemicals which are highly toxic, expensive, and time consuming to prepare. To avoid the use of toxic chemicals and environmental contamination, scientists have developed a simple, rapid method known as "green synthesis" of metal nanoparticles using various parts of plants and their extracts as reducing agents for the generation of metal nanoparticles. Green synthesized AgNPs have been prepared from the different parts of plant extracts such as the leaf extracts of *Melia dubia* [42], *Argeria nervosa* [36], *Flemingia wightiana* [43], *Amaranthus viridis* [31], and *Achyranthus aspera* [44]; fruit extracts of *Ficus carica* [1], *Tinospora cordifolia* [45], and *Terminalia belarica* [46]; and insectivorous plant extract of *Drosera spatulata* [35], and all these AgNPs have a similar SPR band in the range of 410–450 nm comparable to that of the biosynthesized AgNPs in this study. The results are shown in Table 1.

FTIR analysis of biosynthesized Sm-AgNPs

FTIR spectroscopy is a unique technique which is used to obtain infrared spectra of absorption,

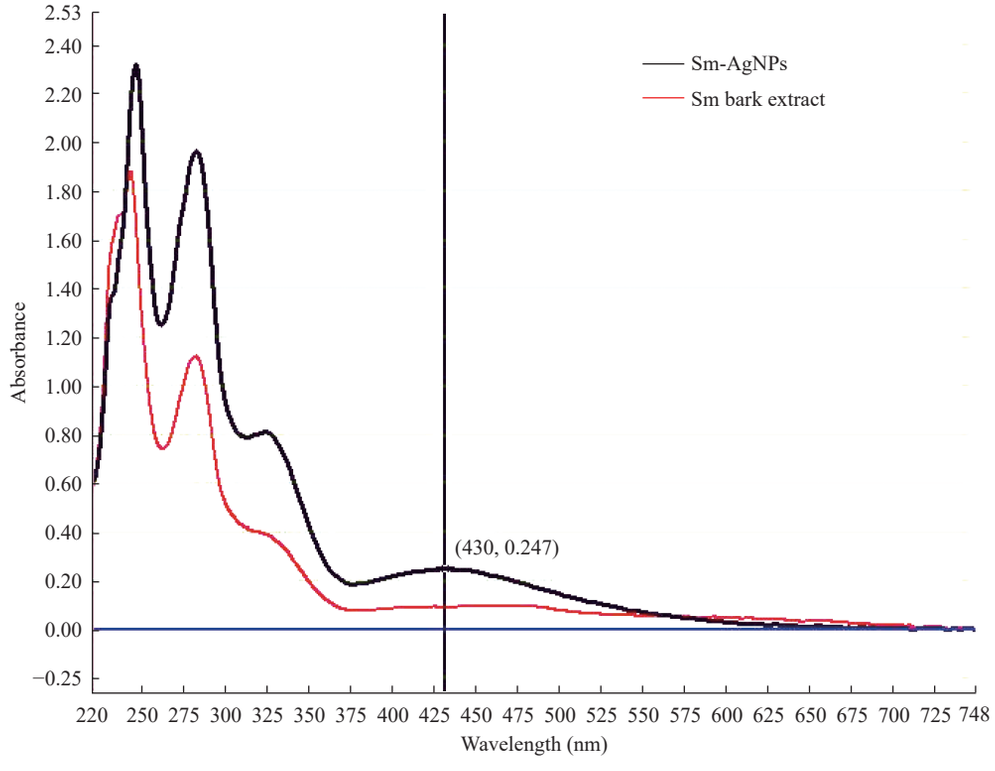

Fig. 3 UV–Vis spectra of *S. mahagoni* bark extract and Sm-AgNPs.

Table 1 Comparison of SPR and size of AgNPs by various plant extracts

Plant	Plant source	Method	SPR band (nm)	Size (nm)	References
M. dubia	Leaf	Green synthesis	380–450	20–40	[42]
A. nervosa	Leaf	Green synthesis	421	10–50	[36]
F. wightiana	Leaf	Green synthesis	380, 460	20–40	[43]
A. viridis	Leaf	Green synthesis	422	55.8	[31]
A. aspera	Leaf	Green synthesis	445	20–40	[44]
F. carica	Fruit	Green synthesis	446	(10 ± 5)–(35 ± 5)	[1]
T. cordifolia	Fruit	Green synthesis	431, 421	30–(35 ± 1), 30–(35.8 ± 1)	[45]
T. belarica	Fruit	Green synthesis	430	46.5	[46]
D. spatulata	Whole plant	Green synthesis	427	23 ± 2	[35]
S. Mahagoni	Bark	Green synthesis	430	35.8–47.8	Present study

emission, and photoconductivity of solids and colloidal solutions. FTIR analyses of the bark extract of *S. mahagoni* and green synthesized Sm-AgNPs are shown in Figs. 4(a) and 4(b). The bark extract of *S. mahagoni* exhibited FTIR peaks at 3 904.93, 3 845.05, 3 372.18, 2 956.65, 1 612.63, 1 518.01, 1 434.90, 1 257.52, 1 111.47, 1 038.07, 789.92, 730.56, and 695.26 cm^{-1}. The peak at 3 372.18 cm^{-1} corresponds to the O—H stretching of free hydroxyl alcohols and phenols. The peak at 2 956.65 cm^{-1} represents C═C, and the peak at 1 612.63 cm^{-1} is due to the N—H bond of primary amines and C═ C and stretching of alkenes and aromatic groups. The peak at 1 518.01 cm^{-1} corresponds to the N—H bending of alkyl halides. The peak at 1 434.90 cm^{-1} is due to the stretching of –C═ O in inorganic carbonate. The peaks at 1 257.52 and 1 111.47 cm^{-1} are due to C—O—C of the CO group in lactones. Finally, the peaks at 730.56 and 695.26 cm^{-1} are due to the C—H groups of aromatic C—H bonds. The FTIR analysis of green synthesized Sm-AgNPs revealed several prominent peaks after reduction such as 3 346.67, 1 636.81, 1 023.77, and 634.31 cm^{-1}. The peak at 3 346.67 cm^{-1} is due to the O—H bonds of alcohol and phenols; the intensity of this peak decreased after the addition of Sm-AgNPs compared to that of the bark extract. The peak at 1 636.81 cm^{-1} corresponds to the stretching and bending of N—H by primary amines and alkenes of the aromatic groups. The peak at 1 023.77 cm^{-1} is due to the S═ O stretching of sulfoxide. Finally, the peak at 634.31 cm^{-1} is due to the C—I stretching of aliphatic iodo compounds and C–Br stretching of halo compounds. An analysis of the FTIR data clearly illustrates that different bioactive compounds were present in the aqueous bark extract of *S. mahagoni*, such as flavonoids, antraquinones, phospholipids, alkaloids, phenols, saponins, terpenoids, cardiac glycosides, volatile oils, long chain unsaturated acids, and 45 limonoids (swietenolide, swiemahogin A, and swiemahogin B); these compounds are actively involved in the reduction of silver nitrate to Sm-AgNPs by capping and stabilization. Various other plant materials have been used to synthesize AgNPs by green methods, such as *A. viridis* [31], *D. spatulata* [35], *A. nervosa* [36], *F. wightiana* [43], and fruit extracts of *T. cordifolia* [45] and *T. belarica* [46]; FTIR analysis in these studies also indicates that bioactive components such as flavonoids, tanins, phenols, saponins, terpenoids,

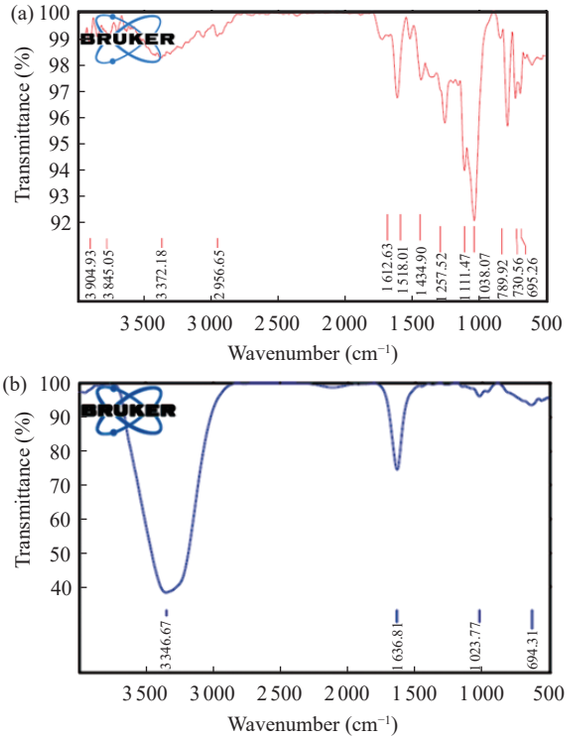

Fig. 4 (a) FTIR analysis of *S. mahagoni* bark extract. **(b)** FTIR analysis of Sm-AgNPs.

phospholipids, alkaloids, glycosides, and proteins are present in the extracts and actively involved in the reduction and stabilization of nanoparticles.

Particle size analysis of green synthesized Sm-AgNPs

The size of green synthesized Sm-AgNPs was detected using the DLS method (Fig. 5(a)). The results reveal that the size of green Sm-AgNPs was in the range of 35.8–47.8 nm with an average mean size of 41.3 nm and a *Z* average of 37.7 nm. This result reveals that 10% of Sm-AgNPs were less than 35.8 nm, 50% were less than 42.8 nm, and 90% were less than 47.8 nm, indicating that green Sm-AgNPs were polydisperse with a polydispersity index (PDI) of 0.169.

Zeta potential analysis of green synthesized Sm-AgNPs

The zeta potential analysis of green Sm-AgNPs reveals that the particles were negatively charged. The net surface charge of green Sm-AgNPs was approximately −19 mV, as shown in (Fig. 5(b)), indicating that these samples were stable

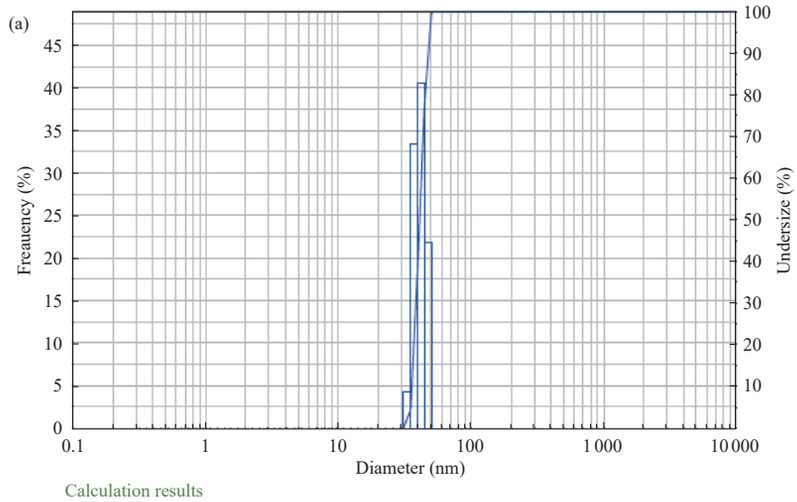

Fig. 5 (a) Particle size (DLS) analysis of Sm-AgNPs. **(b)** Zeta potential analysis of Sm-AgNPs.

nanoparticles in the aqueous colloidal form. Zeta potential is an important physical property which reveals the net surface charge of Sm-AgNPs; this value indicates that the nanoparticles were well dispersed without any agglomeration.

SEM and EDS analysis of green synthesized Sm-AgNPs

The morphology and size of green Sm-AgNPs were observed using SEM, and the size of Sm-AgNPs were in the range of (30 ± 2–50 ± 2) nm with a roughly spherical shape and an average size of (47 ± 2) nm (Fig. 6(a)), which agreed with the DLS data. A similar result was observed in an earlier study [17].

The elemental composition of green Sm-AgNPs was determined using EDS, and the highest proportion peak of Ag was obtained at 3.0 keV, followed by some minor peaks of C, O, and Cu and major peaks of Ag and Si. The high peak of Si is due to depositing Sm-AgNPs on a glass slide. EDS data show the mass percentages of elemental Ag, Cu, C, O, Na, Mg, and Ca were 36.19%, 8.86%, 16.25%, 24.45 %, 14.70%, 11.06%, and 13.72%, respectively (Fig. 6(b)).

Antibacterial activity of green synthesized Sm-AgNPs

The antibacterial activity of green synthesized Sm-AgNPs was determined against both Gram-negative and Gram-positive bacterial strains. The results confirm that green Sm-AgNPs had an exceptionally good antibacterial activity. The ZOI values of Sm-AgNPs against four different bacterial species at amounts of 20, 30, and 40 µg along with those of the bark extract of *S. mahagoni* and standard antibiotic Amoxyclav (30 µg, Himedia-SD063) are shown in Fig. 7, and the ZOI values measured are tabulated in Table 2. Green Sm-AgNPs had a very good antibacterial activity compared with that of 30 µg of Amoxyclav. The bark extract did not have any activity, whereas Sm-AgNPs had an excellent activity with an increase in amount from 20 to 40 µg when compared with that of the standard antibiotic, as shown in Fig. 7. In earlier studies, metal nanoparticles established their antimicrobial activity. Among the metal nanoparticles, AgNPs are known to have an excellent antimicrobial activity against various bacterial species. Presently, several bacterial strains have developed antibiotic resistance due to the prolonged use of antibiotics, which causes a severe illnesses and diseases in humans.

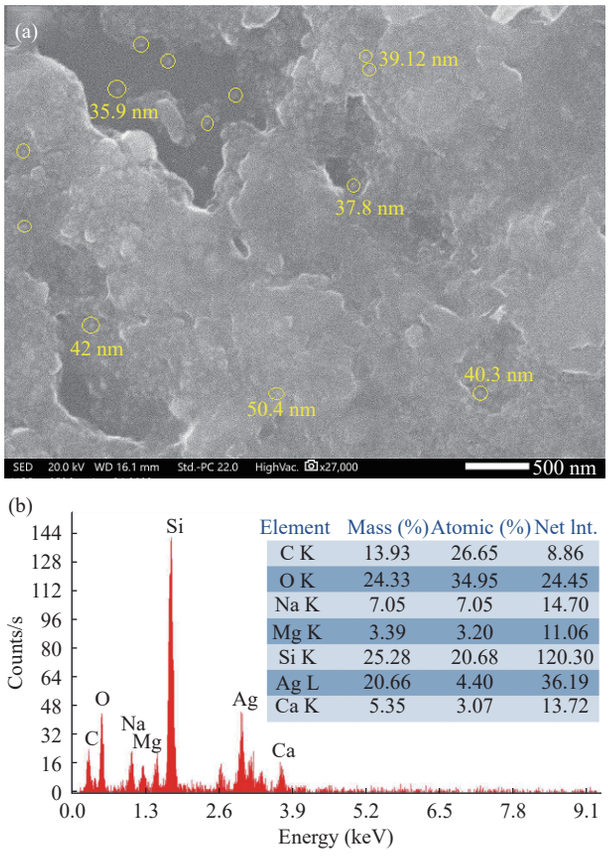

Fig. 6 (a) SEM iamage of sm-AgNPs, **(b)** EDS analysis of Sm-AgNPs.

Therefore, researchers have focused on the development of novel therapeutics agents which can combat antibacterial resistant strains. Several scientists have developed green synthesized AgNPs by using various plant parts such as leaves, roots, fruits, and bark which have an excellent antimicrobial activity. The size and shape of AgNPs play important roles in their antibacterial activity. When AgNPs contact the bacterial cell wall, they attach to the cell wall surface, disturb the cell wall, enter into the bacterial cell, and disturb bacterial cell permeability and respiration. AgNPs induce DNA damage by reactive oxygen species (ROS), which leads to uncontrollable ion transport through the cell membrane. In addition, Ag^{+} ions also bind to tissues and proteins, which precipitates them and obstructs small vessels, leading to bacterial cell death [38, 39]. In conclusion, Sm-AgNPs exhibited a very good antibacterial activity due to their small size from 37 to 49 nm, and nanoparticles are clearly of biomedical importance.

Colorimetric detection of Cr(VI) using green Sm-Ag NPs

The results revealed that the green synthesized colloidal solution of Sm-AgNPs had a strong SPR band.

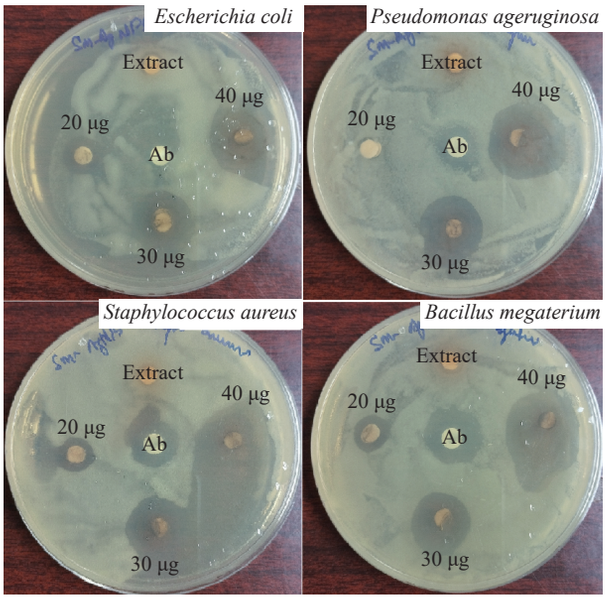

Fig. 7 Antibacterial activity of Sm-AgNPs.

Table 2 Anti microbial activity of Sm-AgNPs

Sample	Extract	ZOI (mm)			
		20 µL (20 µg)	30 µL (30 µg)	40 µL (40 µg)	Antibiotic amoxyclav (30 µg)
E. coli	—	10	16	24	14
P. aeruginosa	—	5	19	23	14
S. aureus	—	11	20	30	12
B. megaterium	—	10	21	26	17

1 mmol/L Cr(VI) stock solution was prepared for this experiment. The maximum optical density (OD) was 8.369 at 360 nm, whereas the maximum absorbance decreased to 2.504 OD after the addition of Sm-AgNPs to the 1 mmol/L Cr(VI) solution, which indicates the interaction of AgNPs with the chromium solution; the color of Cr(VI) changed from orange to dark purple. The results are shown in Fig. 8(a). Similar results were observed using hexavalent chromium (Cr(VI)) and biosynthesized fig fruit (FF)-AgNPs polyvinylprrolidone (PVP-FF-AgNPs) [1], biogenic Pd(0) nanoparticles [47], and AgNPs biosynthesized from a leaf extract of *Anacardium occidentale* [48]. Inorganic nanoparticles act as a catalyst and reducing agent of hexavalent chromium, and the use of inorganic nanomaterials/nanoparticles in the nano-catalyzed reduction of Cr(VI) has attracted a significant attention [49].

Colorimetric sensor detection of Hg^{2+} ions using green Sm-AgNPs

The optical and colorimetric detection of Hg^{2+} ions due to the interaction of Sm-AgNPs with Hg^{2+} ions resulted in a visible color change of Sm-AgNPs from yellow to colorless at high concentrations more than 10 µmol/L (Fig. 8(b)). Further studies at lower concentrations did not produce a visible color change, but an optical change was measured by the UV–Vis spectrophotometer. The disappearance of the characteristic absorption peak of Sm-AgNPs was observed, resulting in a clear solution with zero or nearly zero absorbance intensity. Similar results were observed in starch-functionalized AgNPs which were used to detect Hg^{2+} ions in tap water [50]. Another previous study revealed that cysteine-modified AgNPs can also act as a probe for the selective colorimetric detection of Hg^{2+} [51]. Most studies reported that surface coated or modified AgNPs were used in the colorimetric detection and reduction of Hg^{2+}. In this study, we used unmodified green Sm-AgNPs directly for the colorimetric detection of Hg^{2+}. Unmodified nanoparticles are rarely reported [52]. Therefore, we reported that unmodified green Sm-AgNPs were very efficient in the colorimetric sensing of Hg^{2+}. In future studies, these green Sm-AgNPs can be used as colorimetric probes for sensing different lethal metal ions in environmental samples.

Paper-based sensor detection of Hg^{2+} ions using green Sm-AgNPs

In this study, a Sm-AgNP probe with application to Hg^{2+} sensing was investigated to improve detection in the field. We developed a Whatman filter paper-based sensing strip, and the photographic image shown in Fig. 8(c) exhibited the disappearance of the yellow spots of Sm-AgNPs (sensing line) in contrast to the control sample (control line). Different mercury solution concentrations of 100, 50, 10, 1, 100, 50, 10, and 1 µmol/L were used for the discoloration of Sm-AgNPs. The discoloration was dependent on the Hg^{2+} solution concentrations. Sm-AgNPs spots were colorless after the addition of 5 µL (100 mmol/L), 12 µL (50 mmol/L), 18 µL (10 mmol/L), and 24 µL (1 mmol/L) in the first reaction on Whatman paper, as shown in Fig. 8(c). In addition, a larger volume of Hg^{2+} solution was required at lower concentrations; specifically, 40, 80, 120, and 240 µL volumes required concentrations of 100, 50, 10, and 1 µmol/L, respectively, in the second reaction on Whatman paper (Fig. 8(c)). All the control samples exhibited no visible change in the yellow color of Sm-AgNP spots. Finally, as the concentration of mercury decreased, the required sample volume and discoloration time increased. This result is due to the decreased availability of mercury ions, which decreases the

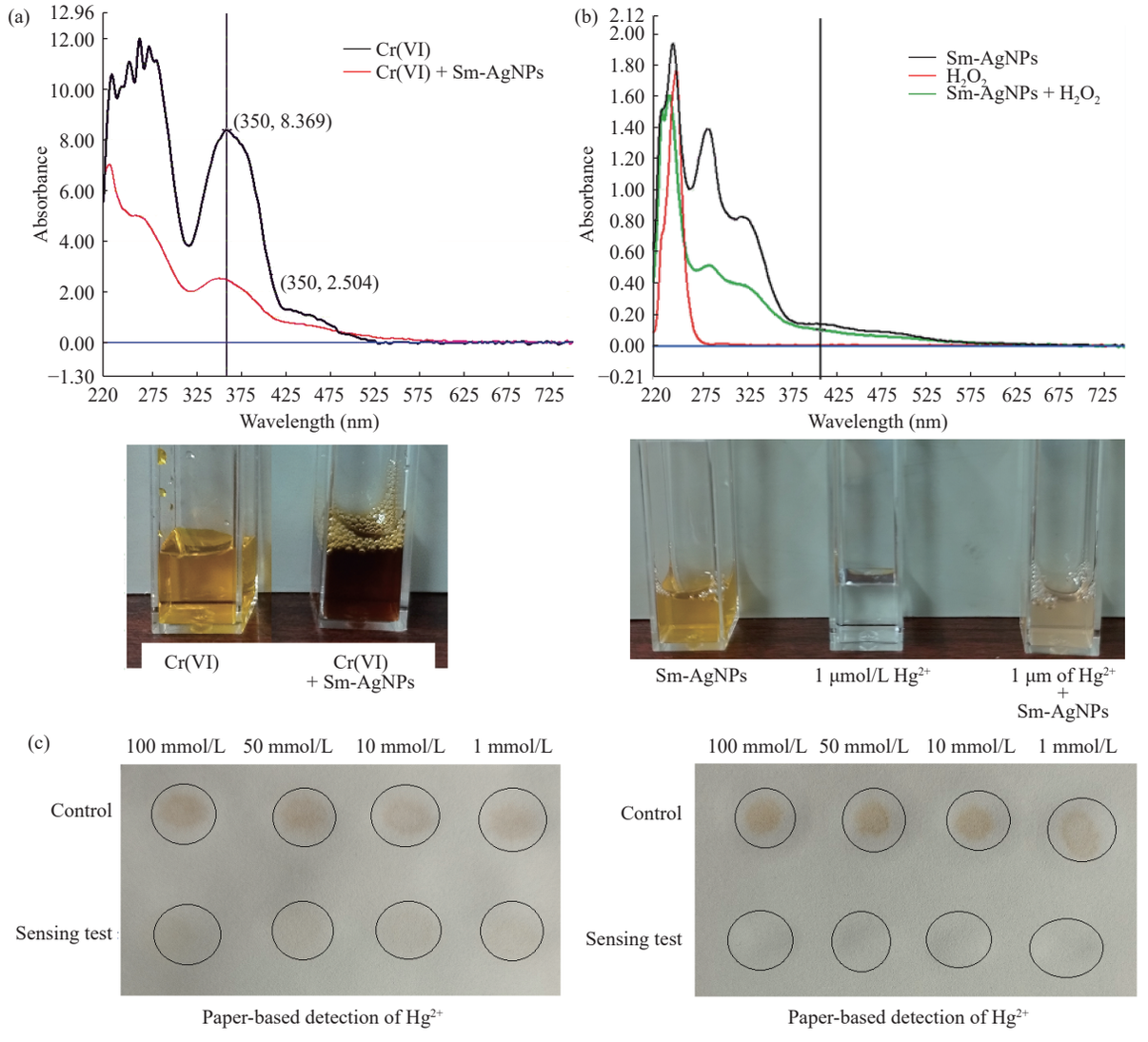

Fig. 8 (a) Colorimetric detection of Cr(VI) using green Sm-AgNPs, **(b)** Colorimetric/optical sensor detection of Hg^{2+} ions using green Sm-AgNPs and **(c)** Paper-based sensor detection of Hg^{2+} ions using green Sm-AgNPs.

reaction rate. The paper-based sensor strip could detect 100 mmol/L of mercury ions within 45 min. A lower concentration of 1 mmol/L required 2 h. Thus, visible detection was easily achieved in the present experiment. Similar results were reported by Nain et al. [16] and Han et al [53]. There are few comparable studies, but a recent study was carried using *Achillea wilhelmsii* extract-mediated silver nanoparticles (Aw-AgNPs) in Hg^{2+} sensing in solution and on a paper substrate [54]. The development of simple paper-based tools will decrease the complexity of sensors and cost of assays, leading to lethal metal samples decreasing to parts per million and parts per billion levels.

Conclusion

In this study, we report a simple and rapid method for the green synthesis of AgNPs using the bark extract of *S. mahagoni*. The results reveal that the green synthesized Sm-AgNPs have important biomedical and industrial applications. The green Sm-AgNPs were characterized by different spectroscopic methods and evaluated in antimicrobial and toxicological applications like dual sensing of Hg^{2+} ions and toxic Cr(VI) reduction. The SPR spectra of Sm-AgNPs were obtained at 430 nm and FTIR analysis revealed that various bioactive molecules of the bark extract actively participated in the reduction and stabilization of Sm-AgNPs. The SEM analysis revealed that Sm-AgNPs were roughly spherical in shape, and EDS data revealed that Sm-AgNPs were completely reduced to elemental silver. The particle size analysis revealed that the green synthesized Sm-AgNPs were polydisperse with an average particle of 41.3 nm, a *Z* average of 37.7 nm, and a PDI of 0.169. The zeta potential of Sm-AgNPs was −19 mV, which

indicates stable colloidal nanoparticles. Furthermore, the green synthesized Sm-AgNPs were evaluated in biomedical and industrial applications, and these materials had a very good antibacterial activity against both Gram-positive and Gram-negative bacteria. These nanoparticles were also useful in the colorimetric detection of Cr(VI) by reduction with Sm-AgNPs. Green Sm-AgNPs proved to be an effective dual sensing agent of Hg^{2+} ions using both optical and paper-based biosensor methods. Finally, Sm-AgNPs can be very useful in the development of novel, simple, and low cost biosensors for the efficient detection of mercury and reduction of chromium.

CRediT Author Statement

Hema Gunti: Methodology, experimental studies, and writing original draft. **Susmila Aparna Gaddam:** Design and plan of study, review, and editing. **Ramamurthy Nadipi:** Experimental studies and results analysis. **Venkata Subbaiah Kotakadi:** Conceptualization, supervision, final manuscript writing, and editing.

Conflict of Interest

The authors declare that no competing interest exists.

References

[1] R.J. Narjala, S.A. Gaddam, S.C. Casimeer, et al. Dual degradation of hexavalent chromium (VI) and cotton blue dye by reduced and PVP-capped silver nanoparticles using fruit extract of *Ficus carica*. *Nano Biomedicine and Engineering*, 2022, 14(2): 123−135. https://doi.org/10.5101/nbe.v14i2.p123-135

[2] B. Rani, S. Punniyakoti, N.K. Sahu. Polyol asserted hydrothermal synthesis of SnO_2 nanoparticles for the fast adsorption and photocatalytic degradation of methylene blue cationic dye. *New Journal of Chemistry*, 2018, 42(2): 943−954. https://doi.org/10.1039/C7NJ03341A

[3] M.A. Brown, S.C. de Vito. Predicting azo dye toxicity. *Critical Reviews in Environmental Science and Technology*, 1993, 23(3): 249−324. https://doi.org/10.1080/10643389309388453

[4] H. Aslani, T. Ebrahimi Kosari, S. Naseri, et al. Hexavalent chromium removal from aqueous solution using functionalized chitosan as a novel nano-adsorbent: Modeling and optimization, kinetic, isotherm, and thermodynamic studies, and toxicity testing. *Environmental Science and Pollution Research International*, 2018, 25(20): 20154−20168. https://doi.org/10.1007/s11356-018-2023-1

[5] Y.J. Yao, J. Zhang, H. Chen, et al. Ni^0 encapsulated in N-doped carbon nanotubes for catalytic reduction of highly toxic hexavalent chromium. *Applied Surface Science*, 2018, 440: 421−431. https://doi.org/10.1016/j.apsusc.2018.01.123

[6] R. Jobby, P. Jha, A.K. Yadav, et al. Biosorption and biotransformation of hexavalent chromium Cr(VI): A comprehensive review. *Chemosphere*, 2018, 207: 255−266. https://doi.org/10.1016/j.chemosphere.2018.05.050

[7] L. Trasande, P.J. Landrigan, C. Schechter. Public health and economic consequences of methyl mercury toxicity to the developing brain. *Environmental Health Perspectives*, 2005, 113(5): 590−596. https://doi.org/10.1289/ehp.7743

[8] T.W. Clarkson, L. Magos. The toxicology of mercury and its chemical compounds. *Critical Reviews in Toxicology*, 2006, 36(8): 609−662. https://doi.org/10.1080/10408440600845619

[9] R. Puk, J.H. Weber. Critical review of analytical methods for determination of inorganic mercury and methylmercury compounds. *Applied Organometallic Chemistry*, 1994, 8(4): 293−302. https://doi.org/10.1002/aoc.590080404

[10] B. Vallant, R. Kadnar, W. Goessler. Development of a new HPLC method for the determination of inorganic and methylmercury in biological samples with ICP-MS detection. *Journal of Analytical Atomic Spectrometry*, 2007, 22(3): 322−325. https://doi.org/10.1039/b615463h

[11] J.S. Barin, B. Tischer, R.S. Picoloto, et al. Determination of toxic elements in tricyclic active pharmaceutical ingredients by ICP-MS: A critical study of digestion methods. *Journal of Analytical Atomic Spectrometry*, 2014, 29(2): 352−358. https://doi.org/10.1039/c3ja50334h

[12] F.X. Han, W.D. Patterson, Y. Xia, et al. Rapid determination of mercury in plant and soil samples using inductively coupled plasma atomic emission spectroscopy, a comparative study. *Water, Air, and Soil Pollution*, 2006, 170(1): 161−171. https://doi.org/10.1007/s11270-006-3003-5

[13] Y.J. Ding, S.S. Wang, J.H. Li, et al. Nanomaterial-based optical sensors for mercury ions. *TrAC Trends in Analytical Chemistry*, 2016, 82: 175−190. https://doi.org/10.1016/j.trac.2016.05.015

[14] S. Mao, J. Chang, G. Zhou, et al. Nanomaterial-enabled rapid detection of water contaminants. *Small*, 2015, 11(40): 5336−5359. https://doi.org/10.1002/smll.201500831

[15] L. Cui, J. Wu, H. Ju. Electrochemical sensing of heavy metal ions with inorganic, organic and bio-materials. *Biosensors & Bioelectronics*, 2015, 63: 276−286.

[16] A. Nain, S.R. Barman, S. Jain, et al. Dual mechanism-based sensing of mercury using unmodified, heteroepitaxially synthesized silver nanoparticles. *Applied Nanoscience*, 2017, 7: 299−307. https://doi.org/10.1007/s13204-017-0572-0

[17] E. Martinsson, M.A. Otte, M.M. Shahjamali, et al. Substrate effect on the refractive index sensitivity of silver nanoparticles. *The Journal of Physical Chemistry C*, 2014, 118(42): 24680−24687. https://doi.org/10.1021/jp5084086

[18] L. Guo, J.A. Jackman, H.-H. Yang, et al. Strategies for enhancing the sensitivity of plasmonic nanosensors. *Nano Today*, 2015, 10(2): 213−239. https://doi.org/10.1016/j.nantod.2015.02.007

[19] G.V. Ramesh, T.P. Radhakrishnan. A universal sensor for mercury (Hg, Hg(I), Hg(II)) based on silver nanoparticle-embedded polymer thin film. *ACS Applied Materials & Interfaces*, 2011, 3(4): 988−994. https://doi.org/10.1021/am200023w

[20] S. Botasini, G. Heijo, E. Méndez. Toward decentralized analysis of mercury (II) in real samples. A critical review on nanotechnology-based methodologies. *Analytica*

Chimica Acta, 2013, 800: 1−11. https://doi.org/10.1016/j.aca.2013.07.067

[21] J. Duan, H. Yin, R. Wei, et al. Facile colorimetric detection of Hg^{2+} based on anti-aggregation of silver nanoparticles. *Biosensors & Bioelectronics*, 2014, 57: 139−142. https://doi.org/10.1016/j.bios.2014.02.007

[22] N. Ding, H. Zhao, W. Peng, et al. A simple colorimetric sensor based on anti-aggregation of gold nanoparticles for Hg^{2+} detection. *Colloids and Surfaces A*: *Physicochemical and Engineering Aspects*, 2012, 395: 161−167. https://doi.org/10.1016/j.colsurfa.2011.12.024

[23] D. Karthiga, A. Rajeshwari, S. Chakravarty, et al. Determination of mercury(ii) ions in aqueous solution using silver nanorods as a probe. *Analytical Methods*, 2016, 8(18): 3756−3762. https://doi.org/10.1039/c6ay00882h

[24] A. Rajeshwari, D. Karthiga, N. Chandrasekaran, et al. Anti-aggregation-based spectrometric detection of Hg(II) at physiological pH using gold nanorods. *Materials Science & Engineering C*, *Materials for Biological Applications*, 2016, 67: 711−716. https://doi.org/10.1016/j.msec.2016.05.066

[25] C. Orwa, A. Mutua, R. Kindt, et al. *Swietenia mahagoni*. Agroforestree Database: a Tree Reference and Selection Guide Version 4.0, pp. 1–5. http://www.worldagroforestry.org/sites/treedbs/treedatabases.asp. (Accessed 25 December 2022).

[26] K. Divya, H.R. Pradeep, K.K. Kumar, et al. Herbal drug *Swietenia mahagoni* Jacq. – A review. *Global Journal Research on Medicinal Plants & Indigenous Medicine*, 2012, 1(10): 557−567.

[27] Y.P. Naveen, G. Divya Rupini, F. Ahmed, et al. Pharmacological effects and active phytoconstituents of Swietenia mahagoni: A review. *Journal of Integrative Medicine*, 2014, 12(2): 86−93. https://doi.org/10.1016/S2095-4964(14)60018-2

[28] M. Bhurat, S. Bavaskar, A. Agrawal, et al. Swietenia mahagoni Linn. – a phytopharmacological review. *Asian Journal of Pharmaceutical Research*, 2011, 1(1): 1−4.

[29] D.K. Patel, S.K. Prasad, R. Kumar, et al. An overview on antidiabetic medicinal plants having insulin mimetic property. *Asian Pacific Journal of Tropical Biomedicine*, 2012, 2(4): 320−330. https://doi.org/10.1016/S2221-1691(12)60032-X

[30] S. Kadota, L. Marpaung, T. Kikuchi, et al. Constituents of the seeds of Swietenia mahagoni JACQ. I.: Isolation, structures, and ^{1}H- and ^{13}C-nuclear magnetic resonance signal assignments of new tetranortriterpenoids related to swietenine, and swietenolide. *Chemical and Pharmaceutical Bulletin*, 1990, 38(3): 639−651. https://doi.org/10.1248/cpb.38.639

[31] V.S. Kotakadi, B. Kolapalli, S.A. Gaddam, et al. Dual synthesis of silver and iron oxide nanoparticles from edible green Amaranthus viridis and their *in vitro* antioxidant activity and antimicrobial studies. *Current Biotechnology*, 2021, 10(3): 191−203. https://doi.org/10.2174/2211550110666211206101654

[32] M.E.T. Yazdi, M. Modarres, M.S. Amiri, et al. Phyto-synthesis of silver nanoparticles using aerial extract of *Salvia leriifolia* Benth and evaluation of their antibacterial and photo-catalytic properties. *Research on Chemical Intermediates*, 2018, 45: 1105−1116. https://doi.org/10.1007/s11164-018-3666-8

[33] S. Menon, K.S. Shrudhi Devi, R. Santhiya, et al. Selenium nanoparticles: A potent chemotherapeutic agent and an elucidation of its mechanism. *Colloids and Surfaces B*: *Biointerfaces*, 2018, 170(1): 280−292. https://doi.org/10.1016/j.colsurfb.2018.06.006

[34] S.J.P. Jacob, V.L.S. Prasad, S. Sivasankar, et al. Biosynthesis of silver nanoparticles using dried fruit extract of *Ficus carica*-Screening for its anticancer activity and toxicity in animal models. *Food and Chemical Toxicology*, 2017, 109(Pt 2): 951−956. https://doi.org/10.1016/j.fct.2017.03.066

[35] S.A. Gaddam, V.S. Kotakadi, G.K. Subramanyam, et al. Multifaceted phytogenic silver nanoparticles by an insectivorous plant *Drosera spatulata* Labill var. bakoensis and its potential therapeutic applications. *Scientific Reports*, 2021, 11(1): 21969. https://doi.org/10.1038/s41598-021-01281-8

[36] G.K. Subramanyam, S.A. Gaddam, V.S. Kotakadi, et al. (2021). *Argyreia nervosa* (*Samudra pala*) leaf extract mediated silver nanoparticles and evaluation of their antioxidant, antibacterial activity, *in vitro* anticancer and apoptotic studies in KB oral cancer cell lines. *Artificial Cells*, *Nanomedicine*, and *Biotechnology*, 2021, 49(1): 635–650. https://doi.org/10.1080/21691401.2021.1996384

[37] S. Palithya, S.A. Gaddam, V.S. Kotakadi, et al. Green synthesis of silver nanoparticles using flower extracts of *Aerva lanata* and their biomedical applications. *Particulate Science and Technology*, 2021, 40(1): 84−96. https://doi.org/10.1080/02726351.2021.1919259

[38] V.S. Kotakadi, S.A. Gaddam, S.K. Venkata, et al. New generation of bactericidal silver nanoparticles against different antibiotic resistant *Escherichia coli* strains. *Applied Nanoscience*, 2015, 5: 847−855. https://doi.org/10.1007/s13204-014-0381-7

[39] V.S. Kotakadi, S.A. Gaddam, S.K. Venkata, et al. Ficus fruit-mediated biosynthesis of silver nanoparticles and their antibacterial activity against antibiotic resistant *E. coli* strains. *Current NanoScience*, 2015, 11(4): 527−538. https://doi.org/10.2174/1573413711666150126225951

[40] C.K. Balavigneswaran, T. Sujin Jeba Kumar, R. Moses Packiaraj, et al. Rapid etection of Cr(VI) by AgNPs probe produced by *Anacardium occidentale* fresh leaf extracts. *Applied Nanoscience*, 2014, 4: 367−378. https://doi.org/10.1007/s13204-013-0203-3

[41] P. Vasileva, T. Alexandrova, I. Karadjova. Application of starch-stabilized silver nanoparticles as a colorimetric sensor for mercury(II) in 0.005 mol/L nitric acid. *Journal of Chemistry*, 2017, 2017: 6897960. https://doi.org/10.1155/2017/6897960

[42] V.R. Netala, V.S. Kotakadi, S.B. Ghosh, et al. Biofabrication of silver nanoparticles using aqueous laef extract of *Melia dubia*, characterization and antifungal activity. *International Journal of Pharmacy and Pharmaceutical Sciences*, 2014, 6(10): 298−300.

[43] N.V. Reddy, B.M. Satyanarayana, S. Sivasankar, et al. Eco-friendly synthesis of silver nanoparticles using leaf extract of *Flemingia wightiana*: spectral characterization, antioxidant and anticancer activity studies. *SN Applied Sciences*, 2020, 2: 884. https://doi.org/10.1007/s42452-020-2702-7

[44] P. Bobbu, V.R. Netala, A.S. Reddy, et al. Rapid synthesis of silver nanoparticles using aqueous leaf extract of *Achyranthes aspera* and study of their antimicrobial and free radical scavenging activities. *International Journal of Pharmacy and Pharmaceutical Sciences*, 2016, 8(5): 341−346.

[45] P. Kanagala, S.A. Gaddam, P. Gunji, et al. Synthesis of bio-inspired silver nanoparticles by ripe and unripe fruit extract of *Tinospora cordifolia* and its antioxidant, antibacterial and catalytic studies. *Nano Biomedicine and Engineering*, 2020, 12(3): 214−226. https://doi.org/10.5101/nbe.v12i3.p214-226

[46] V.S. Kumaram, S.A. Gaddam, V.S. Kotakadi, et al. Multifunctional silver nanoparticles by fruit extract of *Terminalia belarica* and their therapeutic applications: A 3-in-1 system. *Nano Biomedicine and Engineering*, 2018,

10(3): 279−274. https://doi.org/10.5101/nbe.v10i3.p279-294

[47] R.M. Tripathi, S.J. Chung. Reclamation of hexavalent chromium using catalytic activity of highly recyclable biogenic Pd(0) nanoparticles. *Scientific Reports*, 2020, 10(1): 640. https://doi.org/10.1038/s41598-020-57548-z

[48] C.K. Balavigneswaran, T. Sujin Jeba Kumar, R. Moses Packiaraj, et al. Rapid detection of Cr(VI) by AgNPs probe produced by *Anacardium occidentale* fresh leaf extracts. *Applied Nanoscience*, 2014, 4: 367−378. https://doi.org/10.1007/s13204-013-0203-3

[49] Z.H. Farooqi, M.W. Akram, R. Begum, et al. Inorganic nanoparticles for reduction of hexavalent chromium: Physicochemical aspects. *Journal of Hazardous Materials*, 2021, 402: 123535. https://doi.org/10.1016/j.jhazmat.2020.123535

[50] N.M. Abbasi, M.U. Hameed, N. Nasim, et al. Plasmonic nano silver: An efficient colorimetric sensor for the selective detection of Hg^{2+} ions in real samples. *Coatings*, 2022, 12(6): 763. https://doi.org/10.3390/coatings12060763

[51] M. Nidya, M. Umadevi, B.J.M. Rajkumar. Structural, morphological and optical studies of l-cysteine modified silver nanoparticles and its application as a probe for the selective colorimetric detection of Hg^{2+}. *Spectrochimica Acta Part A*, *Molecular and Biomolecular Spectroscopy*, 2014, 133: 265−271. https://doi.org/10.1016/j.saa.2014.04.193

[52] Y. Wang, F. Yang, X.R. Yang. Colorimetric detection of mercury(II) ion using unmodified silver nanoparticles and mercury-specific oligonucleotides. *ACS Applied Materials & Interfaces*, 2010, 2(2): 339−342. https://doi.org/10.1021/am9007243

[53] S.I. Han, K.S. Hwang, R. Kwak, et al. Microfluidic paper-based biomolecule preconcentrator based on ion concentration polarization. *Lab on a Chip*, 2016, 16(12): 2219−2227. https://doi.org/10.1039/c6lc00499g

[54] M. Mavaei, A. Chahardoli, A. Fattahi, et al. A simple method for developing a hand-drawn paper-based sensor for mercury; using green synthesized silver nanoparticles and smartphone as a hand-held-device for colorimetric assay. *Global Challenges*, 2021, 5(4): 2000099. https://doi.org/10.1002/gch2.202000099